Mode of ATM-dependent suppression of chromosome translocation

Motohiro Yamauchi*, Keiji Suzuki, Yasuyoshi Oka, Masatoshi Suzuki,

Hisayoshi Kondo, and Shunichi Yamashita[1]

Graduate School of Biomedical Sciences, Nagasaki University, 1-12-4 Sakamoto,

Nagasaki, 852-8523, Japan

*Corresponding author

Email: motoyama@nagasaki-u.ac.jp

Address: Graduate School of Biomedical Sciences, Nagasaki University, 1-12-4

Sakamoto, Nagasaki, 852-8523, Japan

Tel: +81-95-819-7116

Fax: +81-95-819-7117

Abbreviations

ATM: Ataxia telangiectasia mutated

DNA-PK: DNA-dependent protein kinase

DNA-PKcs: DNA-dependent protein kinase catalytic subunit

DSB: DNA double-strand break

IR: Ionizing radiation

NHEJ: Non-homologous end-joining

MMEJ: Microhomology-mediated end-joining

FISH: Fluorescence *in situ* hybridization

WCP-FISH: Whole chromosome painting-fluorescence *in situ* hybridization

BrdU: bromodeoxyuridine

Abstract

It is well documented that deficiency in ataxia telangiectasia mutated (ATM) protein leads to elevated frequency of chromosome translocation, however, it remains poorly understood how ATM suppresses translocation frequency. In the present study, we addressed the mechanism of ATM-dependent suppression of translocation frequency. To know frequency of translocation events in a whole genome at once, we performed centromere/telomere FISH and scored dicentric chromosomes, because dicentric and translocation occur with equal frequency and by identical mechanism. By centromere/telomere FISH analysis, we confirmed that chemical inhibition or RNAi-mediated knockdown of ATM causes 2~2.5-fold increase in dicentric frequency at first mitosis after 2 Gy of gamma-irradiation in G0/G1. The FISH analysis revealed that ATM/p53-dependent G1 checkpoint suppresses dicentric frequency, since RNAi-mediated knockdown of p53 elevated dicentric frequency by 1.5-fold. We found ATM also suppresses dicentric occurrence independently of its checkpoint role, as ATM inhibitor showed additional effect on dicentric frequency in the context of p53 depletion and Chk1/2 inactivation. Epistasis analysis using chemical inhibitors revealed that ATM kinase functions in the same pathway that requires kinase activity of DNA-dependent protein kinase catalytic subunit (DNA-PKcs) to suppress dicentric frequency. From the results in the present study, we conclude that ATM minimizes translocation frequency through its commitment to G1 checkpoint and DNA double-strand break repair pathway that requires kinase activity of DNA-PKcs.

Keywords

Chromosome translocation

Dicentric

Ataxia telangiectasia mutated

1. Introduction

Recurrent chromosome translocation is implicated in a variety of human diseases, including many hematopoietic malignancies and some type of solid cancers, e.g. prostate cancer [1]. Translocation is generated by incorrect repair between DNA double-strand breaks (DSBs) occurring on two or more chromosomes [2]. Translocation can form hyperactivated fusion gene products, e.g. BCR-ABL, or lead to overexpression of protooncogenes, e.g. c-myc, when the coding sequence of a protooncogene is fused to strong enhancer or promoter, e.g. the enhancer of an immunoglobulin gene [1]. Moreover, translocation is inheritable through generations, which means alteration of genetic information and gene expression is stably transduced to progeny cells [1, 2]. Therefore, minimization of translocation formation or its inheritance is critical for genome integrity and ordered expression of transcriptome and proteome.

It is well documented that deficiency of ataxia telangiectasia mutated (ATM) protein is associated with elevated frequency of translocation both in human and mouse models [3-5]. ATM is a serine/threonine kinase which belongs to phosphoinositide 3-kinase (PI3K)-related protein kinase (PIKK) family [6]. ATM plays a pivotal role in cellular and molecular response to DSBs, such as cell cycle checkpoint and DSB repair [6, 7]. In G1 checkpoint, ATM transduces DSB signals to Chk2 and p53 by phosphorylation, and induces transient delay of S phase entry at earlier times and more sustained blockage of S phase entry at later times, respectively [8-10]. In intra-S checkpoint, Chk1, in cooperation with ATM-activated Chk2, is involved in phosphorylation and subsequent degradation of cdc25A, a phosphatase that dephosphorylates and activates cyclin-dependent kinase 2 (cdk2) [8, 9]. There is another

branch of intra-S checkpoint, which is dependent on NBS1, BRCA1 and SMC1 [8, 11]. This pathway also requires ATM-dependent phosphorylation of the above proteins [8, 11]. In G2 checkpoint, both ATM-Chk2 pathway and ataxia-telangiectasia mutated, and Rad3-related (ATR)-Chk1 pathway are required for phosphorylation and cytoplasmic sequestration and/or inhibition of cdc25C, a phosphatase that performs activatory dephosphorylation of cyclin-dependent kinase 1 (cdk1) [8, 9].

Compared to the absolute requirement for cell cycle checkpoint, ATM plays a relatively minor role in DSB repair. It is estimated that ATM contributes to 10-15% of total DSB repair both in G0/G1 and G2 [12, 13]. In G0/G1, ATM is involved in a subset (~10%) of DSB repair by classical non-homologous end-joining (NHEJ), which is dependent on KU70/80 heterodimer, DNA-dependent protein kinase catalytic subunit (DNA-PKcs), and XLF/XRCC4/Ligase IV complex [12, 14]. In G2, ATM is required for DSB end resection, a prerequisite for homologous recombination, which repairs ~15% of total DSBs arising in G2 phase. [13].

As described above, ATM is involved in both checkpoint and DSB repair, however, it remains unknown how ATM utilizes its checkpoint and repair function to minimize translocation frequency. In the present study, we addressed the mechanism of ATM-dependent suppression of translocation frequency.

2. Materials and Methods

2.1. Cell culture, cell cycle synchronization at G0/G1, and irradiation

Normal human diploid primary fibroblasts (HE49) and hTERT-immortalized normal human diploid foreskin fibroblasts (BJ-hTERT) were cultured in minimum essential Eagle's media (MEM) supplemented with 10% fetal bovine serum (Thermo Fisher Scientific, USA). We observed no dicentric chromosomes both in HE49 and BJ-hTERT when we analyzed 100 metaphase cells. For cell cycle synchronization at G0/G1 phase, cells were cultured for at least two weeks from plating of 1 x 10^6 cells or more in a T25 flask (25 cm^2). Cell cycle synchronization was confirmed by immunofluorescence staining of bromodeoxyuridine (BrdU) and phosphorylated histone H3 at Ser10, an S phase and G2/M phase marker, respectively. Gamma-ray irradiation was performed at room temperature (r.t.) in ^{137}Cs gamma-ray irradiator at a dose rate of 1 Gy/min.

2.2. Chemical Inhibitors

ATM inhibitor (KU55933, Calbiochem, Germany), Chk1/2 inhibitor (SB218078, Tocris Bioscience, UK), and DNA-PK inhibitor (NU7441, Tocris Bioscience, UK) were treated at a final concentration of 5 μM, 2.5 μM, and 1 μM, respectively. The efficacy of the above inhibitors, including inhibition of cell cycle checkpoint and/or DSB repair, is well established as described elsewhere [15-17].

2.3. Whole chromosome painting (WCP)-FISH

Probes for WCP-FISH were obtained from Cambio, UK. Before hybridization,

the probes were predenatured at 72 ˚C for ≥30 min in thermal cycler. Cells on slide glass were pretreated for 10 min at r.t. with ethylene glycol bis[succinimidylsuccinate] (EGS, Thermo Fisher Scientific, USA), a protein crosslinker, at a final concentration of 0.2 mM in 1 x PBS^- to make chromosome morphology more resistant to subsequent denaturation by formamide. After brief washing with 1 x PBS^-, cells were permeabilized with 4 x SSC/0.05% Tween 20 for 2 min at r.t. After brief washing with 1 x PBS^-, the slide glass was immersed in 70% formamide/2 x SSC for 3 min at 64.5 ˚C to denature DNA, followed by brief washing in 2 x SSC. After brief drying, 5 μl of predenatured probe solution was applied onto the center of the metaphase spread, and a coverslip was applied on it to avoid drying. Then, the slide glass was incubated on preheated plate (80 ˚C) for 3 min, and hybridization was performed for ≥2 hr at 37 ˚C in a dark humidified incubator. After hybridization, the slide glass was washed twice with 50% formamide/1 x SSC, then, washed twice with 1 x SSC, followed by washing once with 4 x SSC/0.05% Tween 20. The washing was performed at 42 ˚C. After washing, biotin-labeled probes were fluorescently labeled with strepavidin-Cy5. Chromosomes were stained with DAPI.

2.4. Centromere/telomere FISH

Peptide nucleic acid (PNA) probes for centromere and telomere were purchased from PANAGENE (Korea). Centromere probes were labeled with Cy3, and telomere probes were labeled with Cy5 or FITC. Both probes were diluted with hybridization buffer (70% formamide, 10% blocking protein, 20 mM maleic acid, 30 mM NaCl), so that the probes' final concentration was 1.6 μg/ml. First, dried slide glass was briefly washed in 1 x PBS^-. Then, the slide glass was immersed in 4% formalin/1 x PBS^- for 2

min, followed by brief washing x 3 in 1 x PBS^-. After brief drying, 10 µl of the above diluted probe solution was applied onto the center of metaphase spread, and a coverslip was applied on it to avoid drying. Then, the slide glass was incubated on preheated plate (80 ˚C) for 3 min, followed by hybridization in a dark box for ≥2 hr. Then, the slide glass was washed 15 min x 2 in 70% formamide/TE buffer, and washed 15 min x 2 in TE buffer/0.15 M NaCl/0.05% Tween 20. Chromosomes were stained with DAPI. All the procedures except denaturation were performed at r.t.

Methods for lentivirus infection, establishment of shRNA-expressing cells, induction of ATM shRNAs, and chromosome sample preparation are presented in Online Supplementary Information.

3. Results and Discussion

3.1. ATM kinase suppresses frequency of translocation and dicentric induced by IR

We used ionizing radiation (IR) to generate chromosome trasnlocation, since IR is a well-established inducer of DSBs and chromosome rearrangements, including translocation [2]. In addition, we irradiated confluent-, G0/G1-synchronized cells because most cells in human body are in G0/G1 phase and translocation is a chromosome-type aberration, which should be formed before DNA replication [2]. We confirmed that cells irradiated in S phase rarely have translocations at first mitosis after IR (Supplementary Fig. 1). We also confirmed G2-irradiated cells have no dicentric, a chromosome aberration which occurs with equal frequency and by identical mechanism to translocation, at first mitosis after IR (data not shown) [18, 19]. First we examined whether chemical inhibition of ATM kinase activity affects translocation frequency (Fig. 1). Confluent normal human primary fibroblasts, which have no spontaneous translocation, were irradiated with 2 Gy of gamma-rays in the presence of ATM inhibitor or its vehicle DMSO, and immediately harvested and replated at low density to allow cell cycle progression to mitosis (data not shown, Fig. 1A). Colcemid (0.1 μg/ml) was treated from immediately after replating to the time of metaphase harvest to accumulate first mitotic cells after IR. ATM inhibitor or DMSO was also treated from immediately after replating to the time of metaphase harvest. Forty-hours after replating, mitotic cells were harvested and analyzed by whole chromosome painting (WCP)-FISH probing chromosome #1~6. Typical images of translocation and dicentric are shown in Fig. 1B. Translocation has a constriction, and dicentric has two constrictions, indicating

that they have one or two centromere(s), respectively (Fig. 1B). We found that ATM inhibition increased frequency of both translocation and dicentric involving chromosome #1~6 by 4~5-fold, and translocation frequency and dicentric frequency are quite similar irrespective of ATM inhibition (Fig. 1C). Moreover, we obtained evidence that ATM kinase can suppress translocation frequency through multiple cell generations as translocation frequency at second mitosis was decreased by 40-50% when ATM kinase activity was restored from first to second mitosis, compared to continuous ATM inhibition until second mitosis (Supplementary Fig. 2). In contrast, dicentric frequency at second mitosis was much lower than at first mitosis irrespective of restoration of ATM activity, which is consistent with the notion that dicentric disappears through cell division (Supplementary Fig. 2) [2]. Based on the results in Fig. 1 and Supplementary Fig. 2, we conclude that at first mitosis after IR, dicentric frequency reflects translocation frequency, and we determined to analyze dicentric to know the frequency of translocation events in a whole genome until first mitosis after IR in the following experiments. Next, we performed centromere/telomere FISH to detect dicentric, because dicentric can be unambiguously detected by two centromere signals between two paired telomere signals (Fig. 2A, right image). Mode of DSB-induced dicentric formation and typical images of normal chromosomes and dicentric detected by centromere/telomere FISH are shown in Fig. 2A. We examined the effect of ATM inhibition or depletion on dicentric frequency in another normal human diploid fibroblasts (BJ-hTERT), which have no spontaneous dicentric (data not shown, Fig. 2B and 2C). We observed approximately two-fold increase in dicentric frequency in ATM-inhibited cells, compared to control (Fig. 2C). We employed doxycycline-inducible shRNA expression system to efficiently deplete ATM protein in

confluent cells (Fig. 2B and 2D, see Supplementary Materials and Methods). We found expression of two independent shRNAs (sh #1 and sh #2) against ATM mRNA also increased dicentric frequency by 2~2.5-fold (Fig. 2C). Based on the results in Fig. 2, we conclude that ATM-dependent suppression of dicentric frequency is mainly attributable to ATM's kinase activity.

3.2. ATM/p53-dependent G1 checkpoint contributes to suppression of dicentric frequency

To dissect ATM's checkpoint role in suppression of dicentric frequency, we examined the effect of RNAi-mediated knockdown of p53, because p53 is a critical downstream effector of ATM to induce and sustain G1 checkpoint after IR [8, 9]. Indeed, p53 shRNA blocked 2 Gy-induced G1 arrest similarly to ATM inhibitor (cf. Fig. 3A and 3B). Efficient knockdown of p53 by shRNA was confirmed by western blotting (Fig. 3C). Confluent normal human fibroblasts (BJ-hTERT) expressing either control shRNA (shRNA against EGFP mRNA) or p53 shRNA were irradiated with 2 Gy, and after release from synchronization, first mitotic cells were harvested and analyzed by centromere/telomere FISH (Fig. 3D). The FISH analysis revealed that p53 depletion caused approximately 1.5-fold increase in dicentric frequency, compared to control (Fig. 3E). We also examined the effect of abrogation of G1 checkpoint maintenance on frequency of translocation and dicentric (Supplementary Fig. 3). Transfection of p53 siRNA immediately after irradiation was sufficient to abrogate G1 checkpoint maintenance, because BrdU incorporation of 2 Gy-irradiated cells recovered to control level by 40 hr after irradiation (Supplementary Fig. 3A-C). The delayed p53 depletion

increased dicentric frequency by approximately 1.5-fold (Supplementary Fig. 3D). We also performed WCP-FISH for chromosome #1~6 using the same sample as in Supplementary Fig. 3D, and found the delayed p53 knockdown elevates frequency of both translocation and dicentric (Supplementary Fig. 3E). Further, we obtained evidence that p53 arrests only dicentric-positive cells with unrepaired DSBs, such as terminal deletion or acentric fragments lacking telomere signals, because p53 shRNA increased percentage of dicentric-positive cells with such unrepaired DSBs by >3-fold, compared to control shRNA, while the p53 depletion did not affect percentage of dicentric-positive cells without unrepaired DSBs (Supplementary Fig. 4). In contrast to p53-dependent G1 checkpoint, Chk1/2-dependent intra-S, and G2 checkpoint do not seem to impact on dicentric frequency at least in our system (G0/G1-irradiation, release from synchronization, and analysis of first mitosis after IR), because Chk1/2 inhibitor did not affect dicentric frequency in the context of p53 depletion (Fig. 3F). From the same reason, it seems unlikely that Chk2-dependent transient delay of S phase entry at early times after IR affects dicentric frequency [8-10]. Based on the results in Fig. 3 and Supplementary Fig. 3-4, we conclude that ATM/p53-dependent G1 checkpoint contributes to suppression of dicentric frequency at first mitosis after IR.

3.3. ATM suppresses dicentric frequency in the same pathway as DNA-PKcs.

We noticed that dicentric frequency in ATM-inhibited cells or ATM-depleted cells is reproducibly higher than that in p53-depleted cells (cf. Fig. 2C and Fig. 3E). To know whether ATM also suppresses dicentric frequency independently of its checkpoint role, we examined the effect of ATM inhibition on dicentric frequency in the presence of p53 shRNA and Chk1/2 inhibitor. Confluent BJ-hTERT cells expressing p53 shRNA were

irradiated with 2 Gy in the presence of either Chk1/2 inhibitor alone or Chk1/2 inhibitor and ATM inhibitor (Fig. 4A). Immediately after irradiation, cells were replated at low density and were cultured for 40 hr in the presence of either colcemid/Chk1/2 inhibitor, or colcemid/Chk1/2 inhibitor/ATM inhibitor, followed by metaphase harvest and centromere/telomere FISH analysis (Fig. 4A). We found that ATM inhibitor slightly but reproducibly increased dicentric frequency in the context of p53 depletion and Chk1/2 inactivation, indicating that ATM has some role in suppressing occurrence of dicentric independently of p53/Chk1/Chk2-dependent cell cycle checkpoints (Fig. 4B). It is reported that inactivation of classical NHEJ by knockout of KU70, XRCC4, or Ligase IV leads to elevated frequency of chromosome translocation [20-22]. Therefore, we reasoned that ATM cooperates with classical NHEJ factors to suppress occurrence of translocation. To test this, we used chemical inhibitors for ATM and DNA-PKcs, a classical NHEJ factor, to analyze epistasis between ATM and DNA-PKcs in suppression of dicentric frequency (Fig. 4C). In the presence of p53 shRNA and Chk1/2 inhibitor, chemical inhibition of DNA-PKcs increased dicentric frequency by >2.5-fold, compared to mock-treatment, indicating that kinase activity of DNA-PKcs suppresses dicentric frequency (Fig. 4D left, cf. Fig. 4B, ATM inhibitor (-)). Next we asked whether ATM inhibition shows additional effect on dicentric frequency in the context of DNA-PKcs inhibition (Fig. 4C). We found that ATM inhibition did not affect dicentric frequency in DNA-PKcs-inhibited cells (Fig. 4D). These results indicate that kinase activity of ATM and DNA-PKcs functions in a common pathway to suppress dicentric frequency.

It is well established that kinase activity of DNA-PKcs is crucial for DSB repair by classical NHEJ, however, to our knowledge, this is the first study to demonstrate that

kinase activity of DNA-PKcs is essential for suppression of translocation frequency [23]. It is consistent with the previous studies showing that deficiency of other classical NHEJ factors, such as KU70 and XRCC4, causes elevated translocation frequency [21, 22]. Therefore, it is likely that persistence of unrepaired DSBs due to inactivation of classical NHEJ attracts other-, translocation-prone repair activity. Riballo et al. demonstrated that ATM acts in a subset of DSB repair pathway that requires kinase activity of DNA-PKcs [12]. We consider that the epistasis between ATM and DNA-PKcs in DSB repair can explain the epistasis between the two molecules in suppression of dicentric frequency, because they function in a common pathway to minimize unrepaired DSBs, which otherwise are repaired by classical NHEJ-independent-, translocation-prone pathway. We also think that milder repair defect conferred by ATM inhibition can explain milder increase in dicentric frequency compared to DNA-PKcs inhibition, because less DSBs remain unrepaired in ATM-inhibited cells than in DNA-PKcs-inhibited cells [12]. Molecular analysis of translocation breakpoint junction indicates that microhomology-mediated end-joining (MMEJ), which is also called alternative NHEJ, is a major DSB repair pathway that generates translocation [21, 22, 24]. MMEJ requires 5'-3' resection of DSB ends for microhomology search, and it is recently reported that resection factors, such as MRE11 and CtIP, are involved in MMEJ [25-28]. Indeed, Zhang and Jasin reported that CtIP depletion decreases translocation frequency both in wild-type and KU70(-/-) murine ES cells [29]. Therefore, MRE11 and CtIP are the most plausible candidates to perform translocation-prone MMEJ and increase dicentric frequency when ATM is inhibited or depleted. Importantly, ATM is recently shown to suppress MRE11-dependent DSB end resection and MMEJ, and the ATM-dependent suppression of resection requires its

kinase activity [30].

Our study shows that ATM/p53-dependent G1 checkpoint contributes to suppression of dicentric frequency, and p53 arrests dicentric-positive cells with unrepaired DSBs (Fig. 3 and Supplementary Fig. 4). Therefore, ATM/p53-dependent G1 checkpoint stands as a “safeguard”, when classical NHEJ does not work properly and more DSBs are converted to translocation. G1 checkpoint is highly sensitive, which can be induced by a single DSB [31]. We previously showed that growth of an IR-induced focus of checkpoint factors, such as Ser1981-phosphorylated ATM and 53BP1, allows damage signal of a single DSB to be amplified to a sufficient level to elicit G1 checkpoint [32]. Therefore, cells harboring translocation can be arrested if they have only one unrepaired DSB.

Based on lines of evidence presented by us and others described above, it is likely that ATM has a dual role to minimize translocation frequency; one is suppression of translocation-prone repair pathway, e.g. MMEJ, and the other is induction and maintenance of G1 checkpoint in translocation-positive cells with unrepaired DSB(s). We believe that such great contribution to translocation suppression can partly explain why ataxia telangiectasia individuals are predisposed to cancer [6].

Conflict of interest

The authors declare that there are no conflicts of interest.

Acknowledgement

We thank Dr. Robert Weinberg for providing shp53-pLKO.1 puro vector. This work was supported by Global Center Of Excellence (COE) program in Nagasaki University, and Grant-in-Aid for Scientific Research from Japan Society for the Promotion of Science.

References

[1] S. Fröhlin, H. Döhner, Chromosomal abnormalities in cancer, N. Engl. J. Med. 359 (2008) 722-734.

[2] E.J. Hall, A.J. Giaccia, Radiobiology for the radiologist, sixth edition, Lippincott Williams & Wilkins.

[3] P.H. Kohn, J. Whang-Peng, W.R. Levis, Chromosomal instability in ataxia-telangiectasia, Cancer Genet. Cytogenet. 6 (1982) 289-302.

[4] T.L. Kojis, R.A. Gatti, R.S. Sparkes, The cytogenetics of ataxia telangiectasia, Cancer Genet. Cytogenet. 56 (1991) 143-156.

[5] E. Callén, M. Jankovic, S. Difilippantonio, et al., ATM prevents the persistence and propagation of chromosome breaks in lymphocytes, Cell 2007; 130:63-75.

[6] M.F. Lavin, Ataxia-telangiectasia: from a rare disorder to a paradigm for cell signalling and cancer, Nat. Rev. Mol. Cell Biol. 9 (2008) 759-769.

[7] F.A. Derheimer, M.B. Kastan, Multiple roles of ATM in monitoring and maintaining DNA integrity, FEBS Lett 584 (2010) 3675-3681.

[8] J. Lukas, C. Lukas, J. Bartek, Mammalian cell cycle checkpoints: signaling pathways and their organization in space and time, DNA repair 3 (2004) 997-1007.

[9] G. Iliakis, Y. Wang, J. Guan, et al., DNA damage checkpoint control in cells exposed to ionizing radiation, Oncogene 22 (2003) 5834-47.

[10] D. Deckbar, T. Stiff, B. Koch, et al., The limitation of the G_1-S checkpoint, Cancer Res. 70 (2010) 4412-4421.

[11] R. Kitagawa, C.J. Bakkenist, P.J. McKinnon, et al., Phosphorylation of SMC1 is a critical downstream event in the ATM-NBS1-BRCA1 pathway, Genes Dev. 18 (2004) 1423-1438.

[12] E. Riballo, M. Kühne, N. Rief, et al., A pathway of double-strand break rejoining dependent upon ATM, Artemis, and proteins locating to gamma-H2AX foci, Mol. Cell 16 (2004) 715-724.

[13] A. Beucher, J. Birraux, L. Tchouandong, et al., ATM and Artemis promote homologous recombination of radiation-induced DNA double-strand breaks in G2, EMBO J. 28 (2009) 3413-3427.

[14] K. Hiom, Coping with DNA double strand breaks, DNA repair 9 (2010) 1256-1263.

[15] I. Hickson, Y. Zhao, C.J. Richardson, et al., Identification and characterization of a novel and specific inhibitor of the ataxia-telangiectasia mutated kinase ATM, Cancer Res. 64 (2004) 9152-9159.

[16] J.R. Jackson, A. Gilmartin, C. Imburgia, et al., An indolocarbazole inhibitor of human checkpoint kinase (Chk1) abrogates cell cycle arrest caused by DNA damage, Cancer Res. 60 (2000) 566-572.

[17] Y. Zhao, H.D. Thomas, M.A. Batey, et al., Preclinical evaluation of a potent novel DNA-dependent protein kinase inhibitor NU7441, Cancer Res. 66 (2006) 5354-5362.

[18] J.R.K. Savage, D.G. Papworth, Frequency and distribution studies of asymmetrical versus symmetrical chromosome aberrations, Mutat. Res. 95 (1982) 7–18.

[19] B.D. Loucas, M.N. Cornforth, Complex chromosome exchanges induced by gamma rays in human lymphocytes: an mFISH study, Radiat. Res. 155 (2001) 660-671.

[20] C. Zhu, K.D. Mills, D.O. Ferguson, et al., Unrepaired DNA breaks in p53-deficient cells lead to oncogenic gene amplification subsequent to translocations, Cell 109

(2002) 811-821.

[21] D.M. Weinstock, E. Brunet, M. Jasin, Formation of NHEJ-derived reciprocal chromosomal translocations does not require Ku70, Nat. Cell Biol. 9 (2007) 978-981.

[22] D. Simsek, M. Jasin, Alternative end-joining is suppressed by the canonical NHEJ component Xrcc4–ligase IV during chromosomal translocation formation, Nat. Struct. Mol. Biol. 17 (2010) 410-416.

[23] T.A. Dobbs, J.A. Tainer, S.P. Lees-Miller, A structural model for regulation of NHEJ by DNA-PKcs autophosphorylation, DNA Repair 9 (2010) 1307-1314.

[24] D.M. Weinstock, B. Elliott, M. Jasin, A model of oncogenic rearrangements: differences between chromosomal translocation mechanisms and simple double-strand break repair, Blood 107 (2006) 777-780.

[25] M. McVey, S.E. Lee, MMEJ repair of double-strand breaks (director's cut): deleted sequences and alternative endings, Trends Genet. 24 (2008) 529–538.

[26] A. Xie, A. Kwok, R. Scully, Role of mammalian Mre11 in classical and alternative nonhomologous end joining, Nat. Struct. Mol. Biol. 16 (2009) 814-818.

[27] E. Rass, A. Grabarz, I. Plo, et al., Role of Mre11 in chromosomal nonhomologous end joining in mammalian cells, Nat. Struct. Mol. Biol. 16 (2009) 819-824.

[28] M. Lee-Theilen, A.J. Matthews, D. Kelly, et al., CtIP promotes microhomology-mediated alternative end joining during class-switch recombination, Nat. Struct. Mol. Biol. 18 (2011) 75-79.

[29] Y. Zhang, M. Jasin, An essential role for CtIP in chromosomal translocation formation through an alternative end-joining pathway, Nat. Struct. Mol. Biol. 18 (2011) 80-84.

[30] E.A. Rahal, L.A. Henricksen, Y. Li, et al., ATM regulates Mre11-dependent DNA end-degradation and microhomology-mediated end joining, Cell Cycle 9 (2010) 2866-2877.

[31] L.C. Huang, K.C. Clarkin, G.M. Wahl. Sensitivity and selectivity of the DNA damage sensor responsible for activating p53-dependent G1 arrest, Proc. Natl. Acad. Sci. USA 93 (1996) 4827-4832.

[32] M. Yamauchi, Y. Oka, M. Yamamoto, et al., Growth of persistent foci of DNA damage checkpoint factors is essential for amplification of G1 checkpoint signaling, DNA Repair 7 (2008) 405-417.

Figure legends

Figure 1

ATM kinase suppresses frequency of ionizing radiation-induced chromosome translocation and dicentric.

A. Schematic representation of Fig. 1 experiment.

B. Images of translocation and dicentric. Typical images of translocation and dicenric involving chromosome #1 are shown.

C. Effect of ATM inhibition on frequency of translocation and dicentric involving chromosome #1~6. Average number of translocation or dicentric per cell from two independent experiments is shown. Fifty metaphase cells were scored in each experiment. Error bars represent standard deviation. Note that frequency is similar between translocation and dicentric irrespective of ATM inhibition.

Figure 2

Analysis of dicentric frequency by centromere/telomere FISH in ATM-inhibited or depleted cells.

A. Mode of DSB-induced dicentric formation and typical images of normal chromosomes and dicentric detected by centromere/telomere FISH.

B. Schematic representation of Fig. 2C experiments.

C. Effect of ATM inhibition or depletion on dicentric frequency. Average number of dicentric per cell from two independent experiments was shown. Fifty metaphases were scored in each experiment. Error bars represent standard deviation.

D. ATM depletion by doxycycline-inducible shRNA expression system. +Dox indicates treatment of 2 μg/ml doxycycline for 7 days. ATM depletion was confirmed by western blotting.

Figure 3.

ATM/p53-dependent G1 checkpoint suppresses dicentric frequency.

A. Effect of ATM inhibition on IR-induced G1 checkpoint. Confluent BJ-hTERT cells were mock-irradiated or irradiated with 2 Gy in the presence of ATM inhibitor or DMSO, followed by replating at low density into media containing either ATM inhibitor/BrdU (10 μM) or DMSO/BrdU. Forty-hours later, cells were fixed and subjected to immunofluorescence staining for BrdU. Average from two independent experiments is shown, and at least 2000 cells were scored in each sample. Error bars represent standard deviation.

B. Effect of p53 depletion on IR-induced G1 checkpoint. Confluent BJ-hTERT cells expressing p53 shRNA or control shRNA (EGFP shRNA) were mock-irradiated or irradiated with 2 Gy, followed by replating at low density into media containing BrdU. BrdU-positive cells were analyzed as in Fig. 3A.

C. Depletion of p53 protein by shRNA. Depletion of p53 was confirmed by western blotting.

D. Schematic representation of Fig. 3E and 3F experiments.

E. Effect of p53 depletion on dicentric frequency. Average number of dicentric per cell from two independent experiments is shown. Fifty metaphase cells were scored in each experiment. Error bars represent standard deviation.

F. Effect of Chk1/2 inhibitor on dicentric frequency in the context of p53 depletion. Chk1/2 inhibitor was treated from 30 min before IR to the time of metaphase harvest. Analysis and data display were performed as in Fig. 3E.

Figure 4.

ATM suppresses dicentric frequency in the same pathway as DNA-PKcs.

A. Schematic representation of Fig. 4B experiments.

B. Effect of ATM inhibition on dicentric frequency in the context of p53 depletion and Chk1/2 inhibition. Average number of dicentric per cell from two independent experiments is shown. Fifty metaphase cells were scored in each experiment. Error bars represent standard deviation.

C. Schematic representation of Fig. 4D experiments.

D. Effect of DNA-PKcs inhibition or DNA-PKcs/ATM double-inhibition on dicentric frequency in the context of p53 depletion and Chk1/2 inhibition. Average number of dicentric per cell from two independent experiments is shown. Fifty metaphase cells were scored in each experiment. Error bars represent standard deviation.

Fig. 1

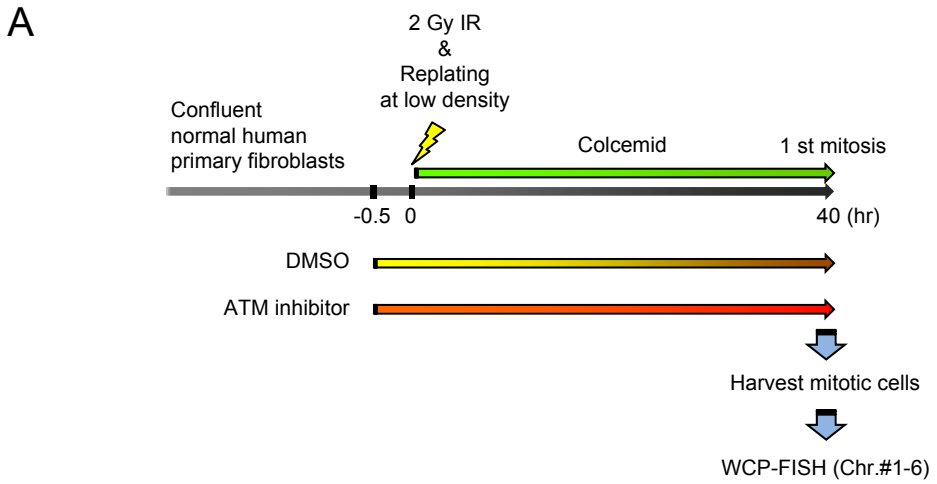
A
2 Gy IR
&
Replating
at low density
Confluent
normal human
primary fibroblasts
Colcemid
1 st mitosis
-0.5
0
40 (hr)
DMSO
ATM inhibitor
Harvest mitotic cells
WCP-FISH (Chr.#1-6)

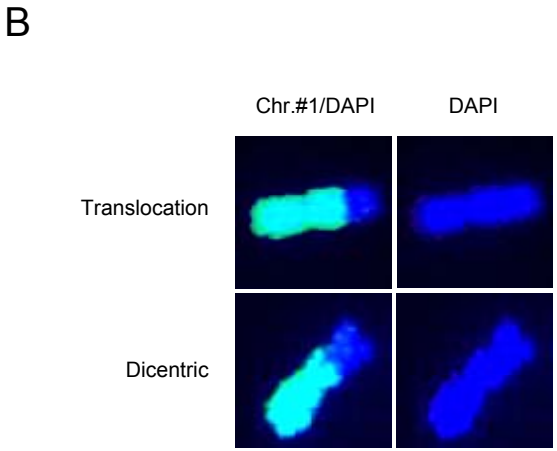
B
Chr.#1/DAPI
DAPI
Translocation
Dicentric

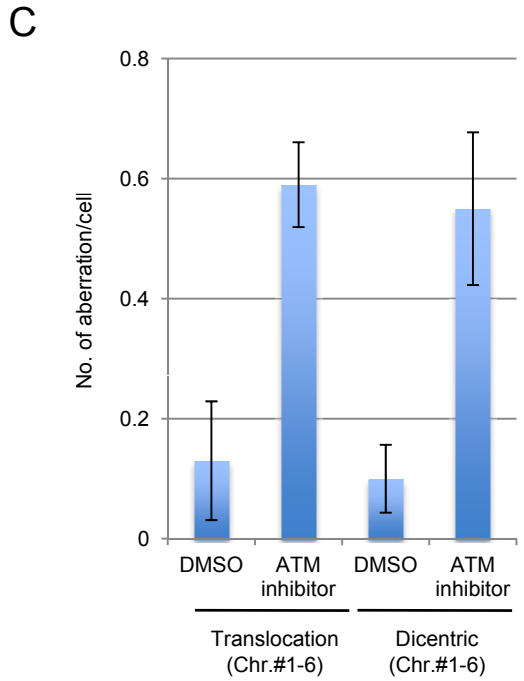
C
No. of aberration/cell
0.8
0.6
0.4
0.2
0
DMSO
ATM inhibitor
DMSO
ATM inhibitor
Translocation (Chr.#1-6)
Dicentric (Chr.#1-6)

Fig. 2

A

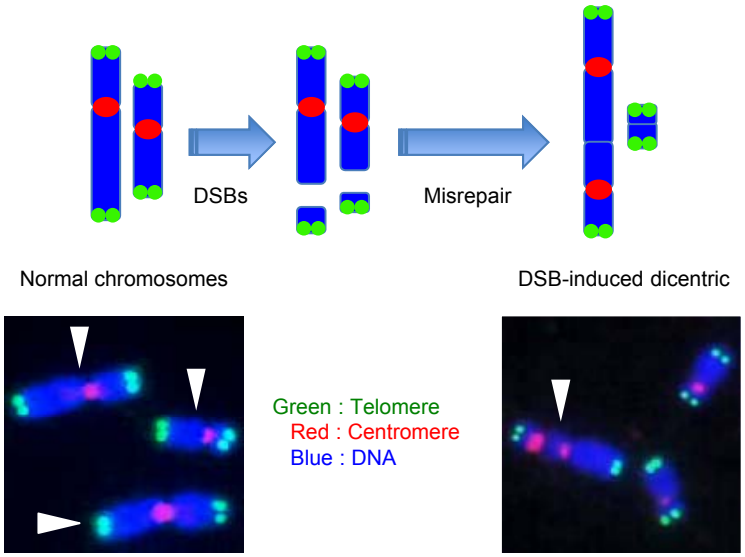
DSBs
Misrepair
Normal chromosomes
DSB-induced dicentric
Green : Telomere
Red : Centromere
Blue : DNA

C

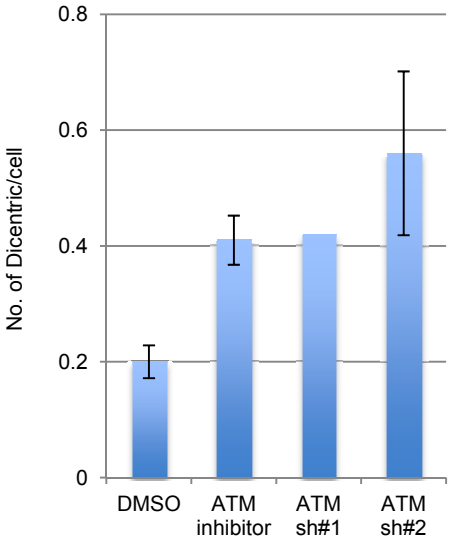
No. of Dicentric/cell
0.8
0.6
0.4
0.2
0
DMSO
ATM inhibitor
ATM sh#1
ATM sh#2

B

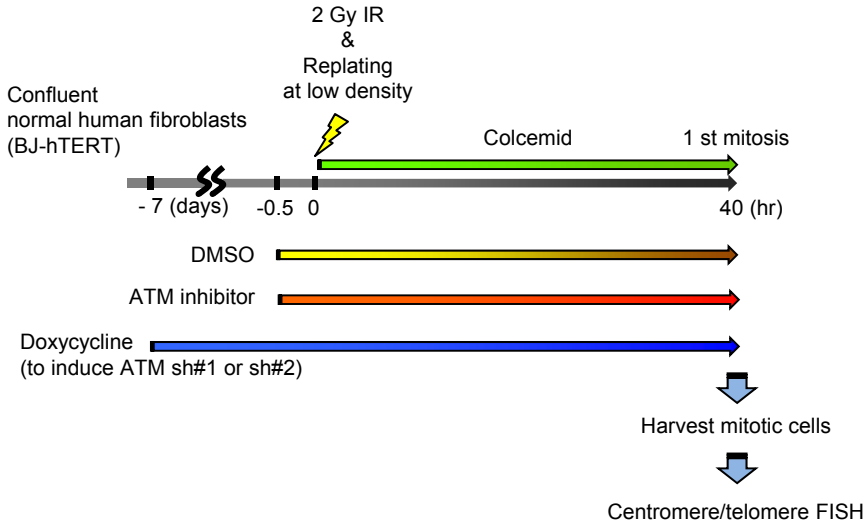
2 Gy IR
&
Replating
at low density
Confluent
normal human fibroblasts
(BJ-hTERT)
Colcemid
1 st mitosis
- 7 (days)
-0.5
0
40 (hr)
DMSO
ATM inhibitor
Doxycycline
(to induce ATM sh#1 or sh#2)
Harvest mitotic cells
Centromere/telomere FISH

D

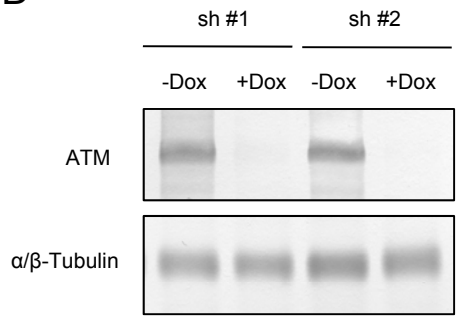
sh #1
sh #2
-Dox
+Dox
-Dox
+Dox
ATM
α/β-Tubulin

Fig. 3

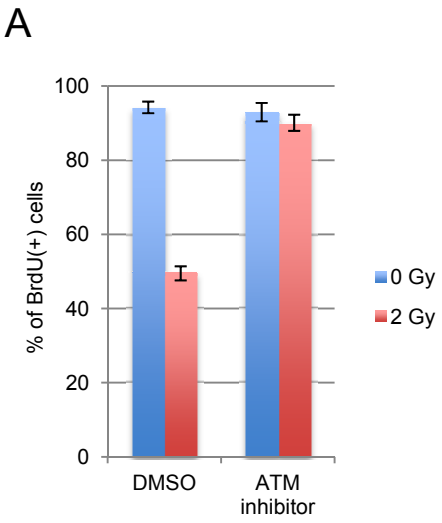
A
100
80
60
40
20
0
% of BrdU(+) cells
0 Gy
2 Gy
DMSO
ATM inhibitor

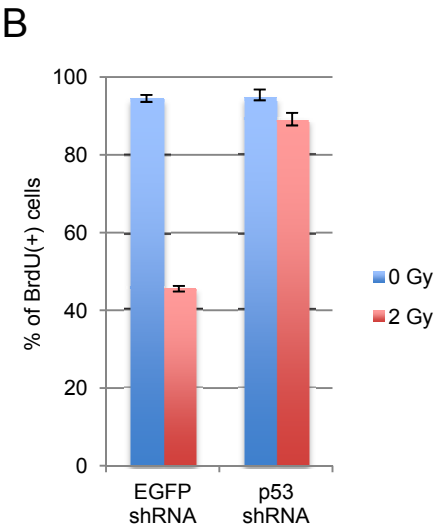
B
100
80
60
40
20
0
% of BrdU(+) cells
0 Gy
2 Gy
EGFP shRNA
p53 shRNA

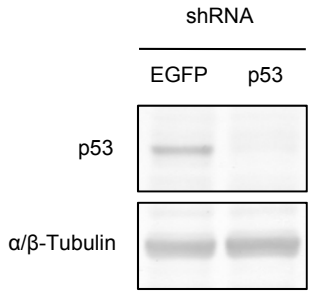
C
shRNA
EGFP
p53
p53
α/β-Tubulin

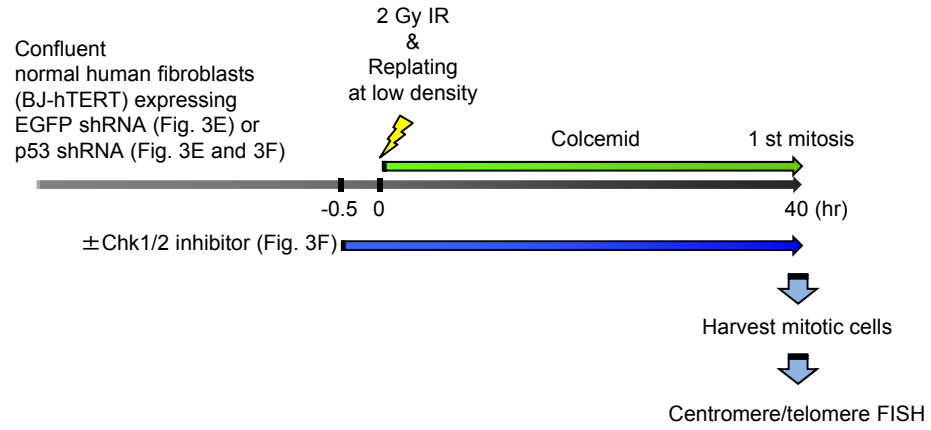
D
Confluent
normal human fibroblasts
(BJ-hTERT) expressing
EGFP shRNA (Fig. 3E) or
p53 shRNA (Fig. 3E and 3F)
2 Gy IR
&
Replating
at low density
Colcemid
1 st mitosis
-0.5
0
40 (hr)
±Chk1/2 inhibitor (Fig. 3F)
Harvest mitotic cells
Centromere/telomere FISH

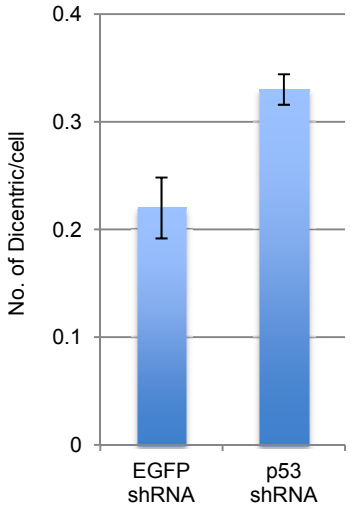
E
0.4
0.3
0.2
0.1
0
No. of Dicentric/cell
EGFP shRNA
p53 shRNA

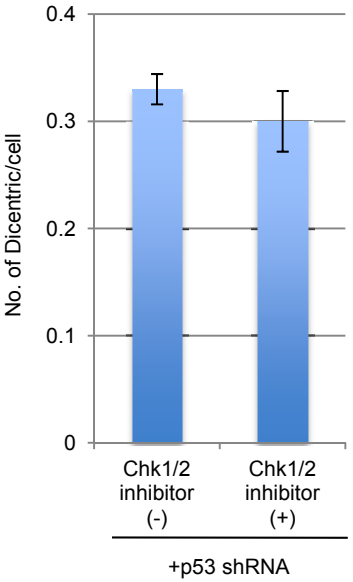
F
0.4
0.3
0.2
0.1
0
No. of Dicentric/cell
Chk1/2 inhibitor (-)
Chk1/2 inhibitor (+)
+p53 shRNA

Fig. 4

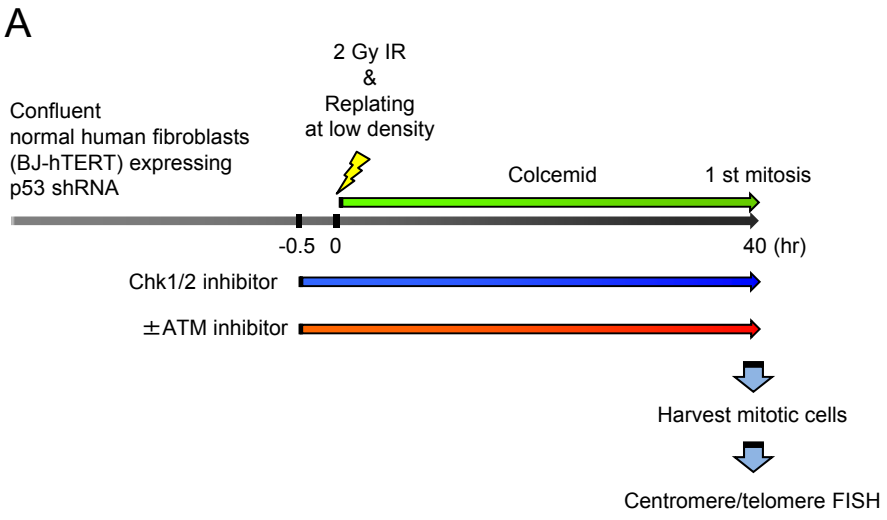
A
2 Gy IR
&
Replating
at low density
Confluent
normal human fibroblasts
(BJ-hTERT) expressing
p53 shRNA
Colcemid
1 st mitosis
-0.5
0
40 (hr)
Chk1/2 inhibitor
±ATM inhibitor
Harvest mitotic cells
Centromere/telomere FISH

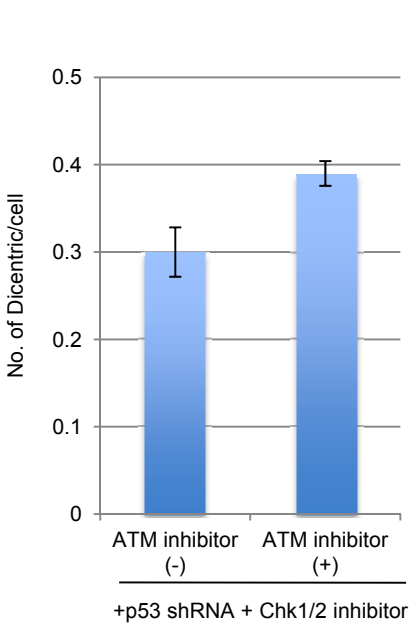
B
No. of Dicentric/cell
0.5
0.4
0.3
0.2
0.1
0
ATM inhibitor
(-)
ATM inhibitor
(+)
+p53 shRNA + Chk1/2 inhibitor

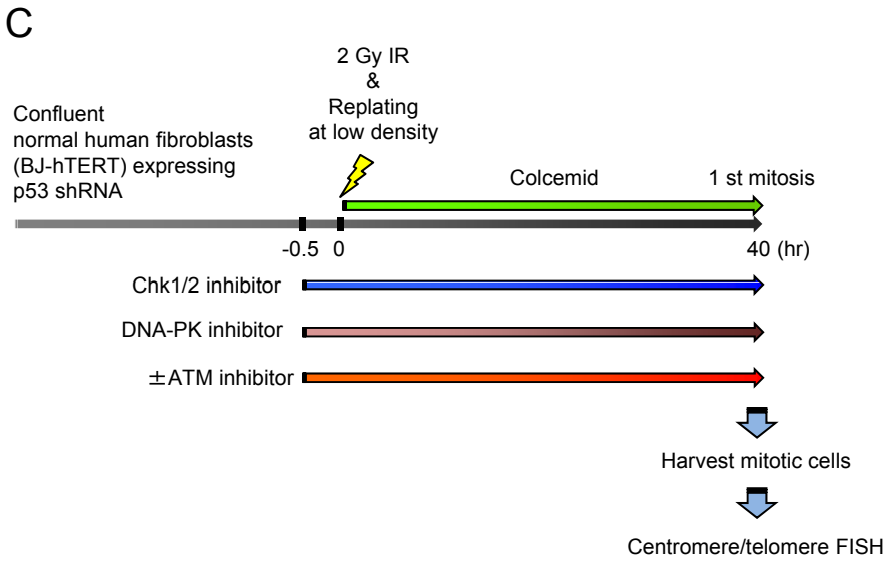
C
2 Gy IR
&
Replating
at low density
Confluent
normal human fibroblasts
(BJ-hTERT) expressing
p53 shRNA
Colcemid
1 st mitosis
-0.5
0
40 (hr)
Chk1/2 inhibitor
DNA-PK inhibitor
±ATM inhibitor
Harvest mitotic cells
Centromere/telomere FISH

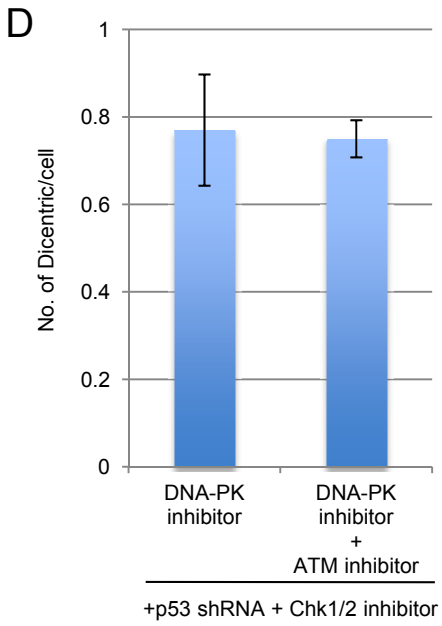
D
No. of Dicentric/cell
1
0.8
0.6
0.4
0.2
0
DNA-PK
inhibitor
DNA-PK
inhibitor
+
ATM inhibitor
+p53 shRNA + Chk1/2 inhibitor

Supplementary Materials and Methods

1. Lentivirus infection, establishment of shRNA-expressing cells, and induction of ATM shRNAs

Lentivirus vectors expressing shRNAs for ATM or enhanced green fluorescent protein (EGFP) were purchased from Thermo Fisher Scientific, USA. Kinds of lentivirus vectors and their clone ID or catalog number are as follows: ATM shRNA #1 (TRIPZ shRNAmir, clone ID V2THS_89368) , ATM shRNA#2 (TRIPZ shRNAmir, clone ID V2THS_192880), EGFP shRNA (pLKO.1, RHS4459). A lentivirus vector expressing p53 shRNA (shp53 pLKO.1 puro) was provided by Dr. Robert Weinberg through Addgene (USA) (Addgene plasmid 19119) [1]. For virus production, shRNA-expressing vector (8 μg) was cotransfected with packaging vector (pCMV-dR8.74, 8 μg) and envelope vector (pMD2.G, 8 μg) into 293T cells (8-9 x 10^6) with Lipofectamine 2000 (Invitrogen), and cells were cultured for 8~10 hr, followed by media change and culture for additional 48 hr. Then, the supernatant of the culture media containing virus was collected and passed through 0.45 μm filter. For virus infection, the filtered supernatant was then either directly treated (for ATM shRNA) or treated with a dilution ratio of 1:10~100 onto cells (for p53 shRNA and EGFP shRNA), which were plated (3 x 10^5 cells/T25 flask) a day before infection. The virus infection was performed for 12-15 hr in humidified CO_2 incubator at 37˚C. After infection, cells were washed twice with 1 x PBS^-, then cultured for 3 days, followed by puromycin selection for 1-2 weeks. Final concentration of puromycin for selection was 15 μg/ml for ATM shRNA-expressing cells, and 1 μg/ml for p53 shRNA-, or EGFP shRNA-expressing cells. ATM shRNAs were induced by treatment of doxycycline (2

μg/ml) for 7 days.

2. Chromosome sample preparation

Confluent cells were irradiated with 2 Gy of gamma-rays and harvested by trypsinization and replated at low density (2~2.5 x 10^6 cells in T75 flask) immediately after irradiation to allow cell cycle progression to mitosis. Colcemid (0.1 μg/ml) was continuously treated from the time of replating to the time of metaphase harvest (40 hr after replating) to accumulate first metaphase cells. Metaphase cells were harvested by brief washing with 1 x PBS^- and trypsin, followed by tapping of a flask. After centrifugation (1,200 rpm, 5 min) of cell suspension and washing by 1 x PBS^-, cells were treated with hypotonic buffer (0.075 M KCl) for 20 min at r.t., followed by fixation with Carnoy's fixative (methanol : acetic acid = 3 : 1) on ice for ≥30 min. After fixation, cells were resuspended with appropriate volume of Carnoy's fixative, and the cell suspension was dropped onto a 70%-ethanol-immersed slide glass. The slide glass was dried for at least 1 day in dessicator (humidity ≤ 30%), and was subjected to whole chromosome painting (WCP)-FISH, or centromere/telomere FISH.

Reference

1. S. Godar, T.A. Ince, G.W. Bell, Growth-inhibitory and tumor- suppressive functions of p53 depend on its repression of CD44 expression, Cell 134 (2008) 62-73.

Supplementary Figure legends

Supplementary Figure 1

Cells irradiated in S phase rarely have translocation or dicentric at first mitosis after irradiation.

A. Schematic representation of Supplementary Figure 1 experiment. S phase cells of exponentially-growing normal human primary fibroblasts were labeled with bromodeoxyuridine (BrdU, 10μM) for 1 hr prior to irradiation. Then, cells were washed with fresh media to remove BrdU, followed by 2 Gy-irradiation in the presence of Chk1/2 inhibitor and ATM inhibitor. Chk1/2 inhibitor and ATM inhibitor were used because otherwise S phase cells cannot progress to mitosis probably due to intra-S, and G2 checkpoint. Colcemid (0.1 μg/ml) was treated for 6 hr before metaphase harvest to accumulate BrdU-positive metaphase cells. Ten hours after irradiation, mitotic cells were harvested and analyzed by centromere/telomere FISH or WCP-FISH probing chromosome #1, 2, and 3.
B. Typical image of BrdU-positive metaphase cells probed by centromere/telomere FISH. BrdU, centromeres, telomeres, and chromosomes were stained green, red, white, and blue, respectively. Note the uneven BrdU staining on chromosomes, indicating that there were both replicated and unreplicated DNA regions at the time of irradiation.
C. Typical image of BrdU-positive metaphase cells probed by WCP-FISH for chromosome #3. BrdU, chromosome #3, and chromosomes were stained green, red, and blue, respectively. Note the uneven BrdU staining on chromosomes, indicating

that there were both replicated and unreplicated DNA regions at the time of irradiation.

D. Frequency of dicentric or translocation involving chromosome #1, 2, or 3. Dicentric or translocated chromosome #1, 2, or 3 in BrdU-positive metaphase cells was analyzed.

Supplementary Figure 2

ATM can suppress translocation frequency through multiple cell generations.

A. Schematic representation of Supplementary Figure 2 experiment. Confluent normal human primary fibroblasts were irradiated with 2 Gy of gamma-rays in the presence of ATM inhibitor, followed by trypsinization and replating at low density into media containing ATM inhibitor. We observed that many cells enter first mitosis 40 hr after replating and second mitosis 72 hr after replating (data not shown). Forty-hours after replating, cells were either washed to remove ATM inhibitor or kept treated with ATM inhibitor, and cultured until 72 hr after replating. Colcemid (0.1 μg/ml) was treated for 6 hr before metaphase harvest. Seventy-two hours after replating, when many cells enter second mitosis, metaphase cells were harvested and analyzed by WCP-FISH probing chromosome #1-6.

B. Effect of restoration of ATM kinase activity on the frequency of translocation and dicentric at second mitosis after G0/G1-irradiation. Average number of translocation or dicentric per cell from two independent experiments is shown. At least 30 metaphase cells were scored in each experiment. The left-most bars indicate frequency of translocation and dicentric at first mitosis after irradiation which is presented in Figure 1C. Note the lower translocation frequency in the population where ATM kinase activity was restored from first mitosis to second mitosis after irradiation, compared to the population where ATM activity was inhibited until second mitosis. Also note the much lower dicentric frequency at second mitosis than at first mitosis, irrespective of restoration of ATM kinase activity.

Supplementary Figure 3

Maintenance of p53-dependent G1 checkpoint is critical for suppression of translocation-, and dicentric frequency.

A. Schematic representation of Supplementary Figure 3D and 3E experiments.

Confluent normal human primary fibroblasts were irradiated with 2 Gy of gamma-rays, and immediately after irradiation, cells were harvested and transfected with either p53 siRNA or control siRNA. Then, cells were replated at low density to allow cell cycle progression to mitosis. Colcemid was treated from immediately after replating to the time of metaphase harvest to accumulate first mitosis after irradiation. Forty-hours after replating, metaphase cells were harvested and analyzed by centromere/telomere FISH in Supplementary Figure 3D and by WCP-FISH probing chromosome #1-6 in Supplementary Figure 3E.

B. Effect of p53 siRNA transfection *after* irradiation on G1 checkpoint maintenance.

Confluent normal human primary fibroblasts were mock-irradiated or irradiated with 2 Gy of gamma-rays, and immediately after irradiation, cells were harvested and transfected with either p53 siRNA or control siRNA. Then, cells were replated at low density into BrdU-containing media to allow cell cycle progression to mitosis. Forty-hours after replating, cells were fixed and subjected to immunofluorescence staining for BrdU. Average from two independent experiments is shown, and at least 2000 cells were scored in each sample. Error bars represent standard deviation. Note that percentage of BrdU-incorporated cells is similar between unirradiated cells and irradiated cells in the presence of p53 siRNA, indicating that p53 siRNA transfection *after* IR is sufficient for abrogation of G1 checkpoint maintenance.

C. Depletion of p53 protein by siRNA. Confluent normal human primary fibroblasts were irradiated with 2 Gy of gamma-rays, and immediately after irradiation, cells were harvested and transfected with either p53 siRNA or control siRNA. Then, cells were replated at similar density to Supplementary Figure 3D and 3E experiments, and forty-hours later, total cellular proteins were collected and subjected to western blotting for p53 and α/β-tubulin.

D. Effect of delayed p53 depletion on dicentric frequency. Average number of dicentric per cell from two independent experiments is shown. Fifty metaphase cells were scored in each experiment. Error bars represent standard deviation. Note that the p53 siRNA transfection *after* irradiation increased dicentric frequency similarly to constitutive p53 depletion from before irradiation in Fig. 3E (both ways of p53 depletion caused approximately 1.5 fold increase in dicentric frequency).

E. Effect of delayed p53 depletion on frequency of translocation and dicentric involving chromosome #1~6. The same samples as in Supplementary Fig. 3D were analyzed by WCP-FISH probing chromosome #1~6. Analysis and data display were performed as in Fig. 1C.

Supplementary Figure 4

p53 suppresses dicentric-positive cells with unrepaired DSBs to progress to mitosis.

A. Typical images of chromosome aberrations detected by centromere/telomere FISH. In centromere/telomere FISH, a normal chromosome has a centromere signal and two paired telomere signals at both chromosome ends as indicated in Fig. 2A. Therefore, in the analysis of Supplementary Figure 4B, chromosomes or acentric fragments lacking telomere signal(s), such as terminal deletion or acentric fragment with ≤ 3 telomeres were regarded as unrepaired DSBs. Acentric fragments with 4 telomeres were regarded as repaired DSBs.

B. Frequency of dicentric-positive cells with or without unrepaired DSBs in p53-depleted cells. The same chromosome samples as in Fig. 3E were analyzed. Percentage of dicentric-positive cells with or without unrepaired DSBs, which are defined in Supplementary Figure 4A, is shown. Average percentage from two independent experiments is indicated, and 50 metaphase cells were scored in each experiment. Note that p53 depletion increased only dicentric-positive cells with unrepaired DSBs, while percentage of dicentric-positive cells without unrepaired DSBs was unaffected by p53 depletion.

Supplementary
Fig. 1

A

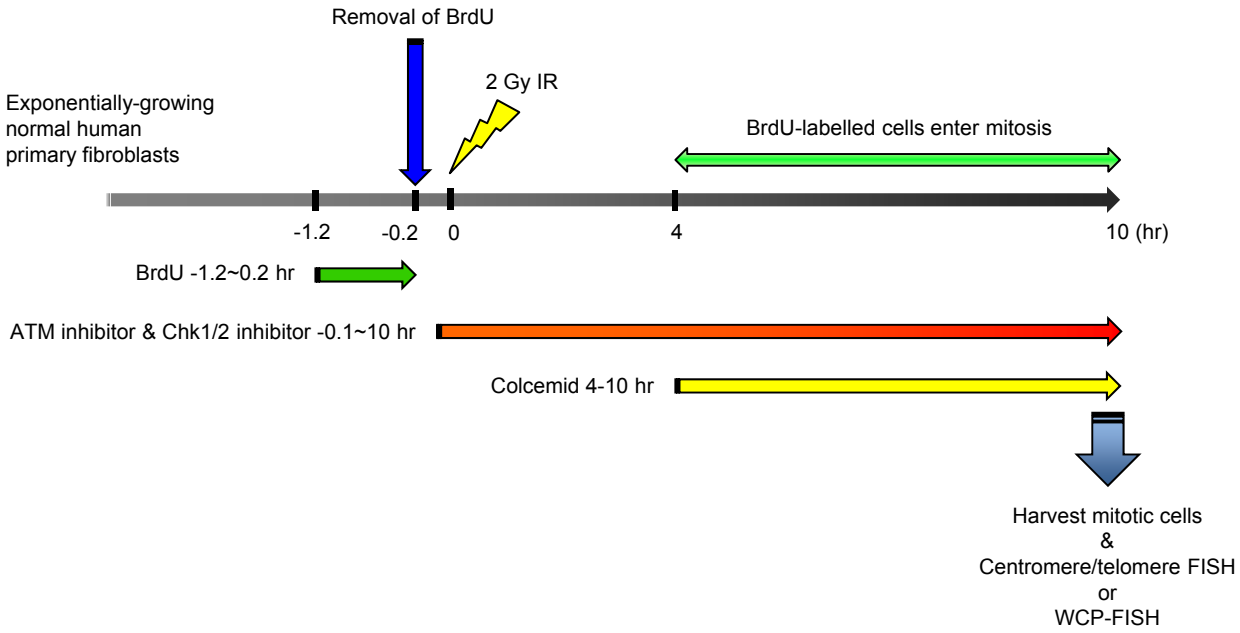

B

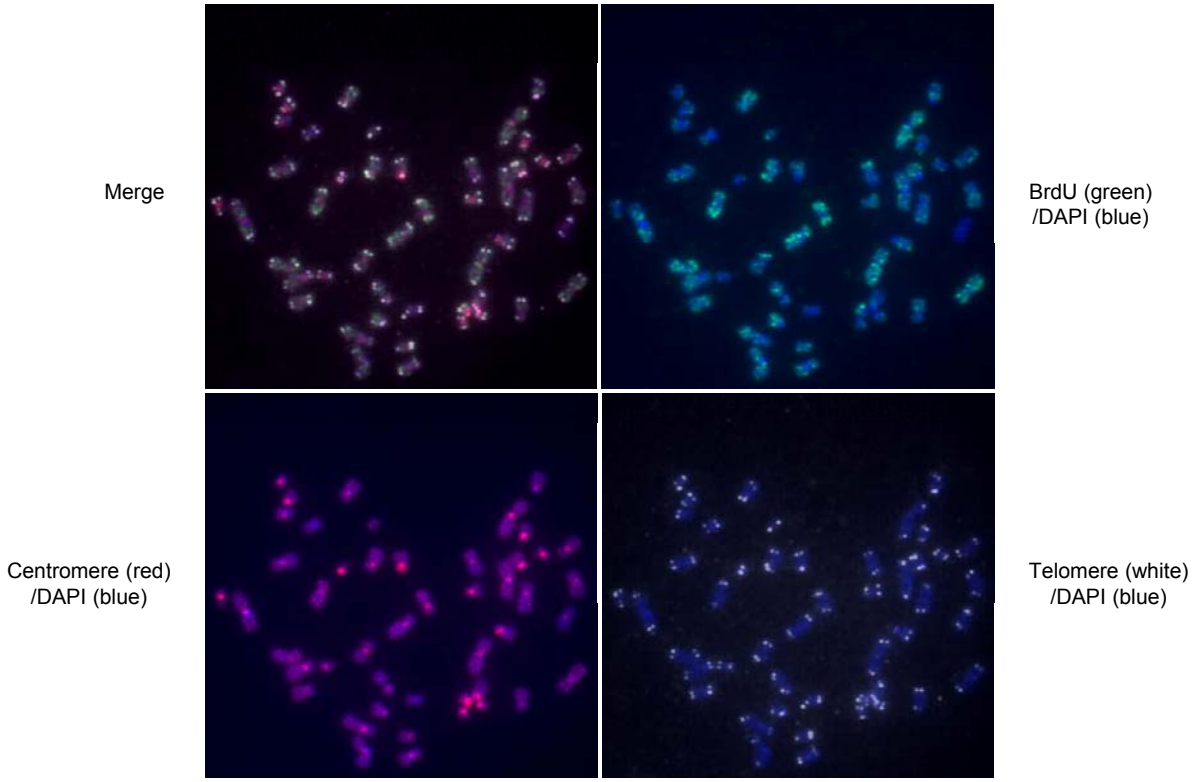

Supplementary Fig. 1

C

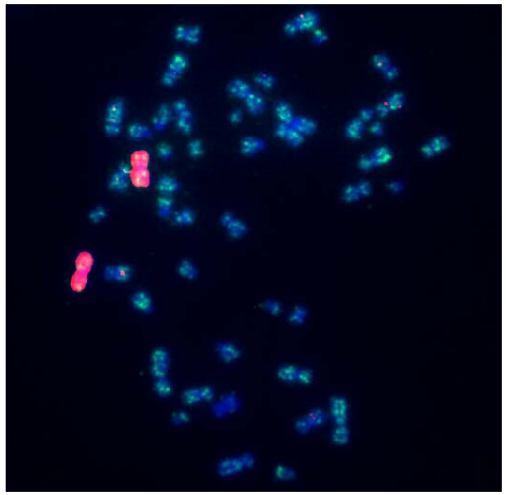

BrdU (green)
/Chr. #3 (red)
/DAPI (blue)

D

	No. of BrdU (+) metaphases analyzed	No. of dicentric or translocation
Centromere/Telomere FISH	51	1
WCP-FISH for Chr. #1	81	1
WCP-FISH for Chr. #2	82	0
WCP-FISH for Chr. #3	69	1

Supplementary Fig. 2

A

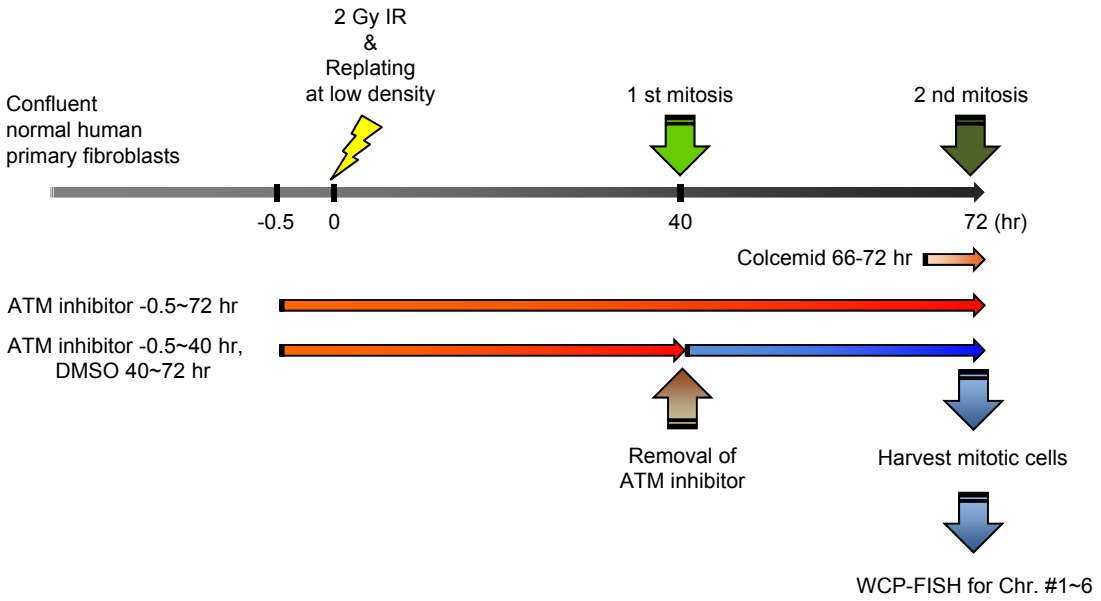

B

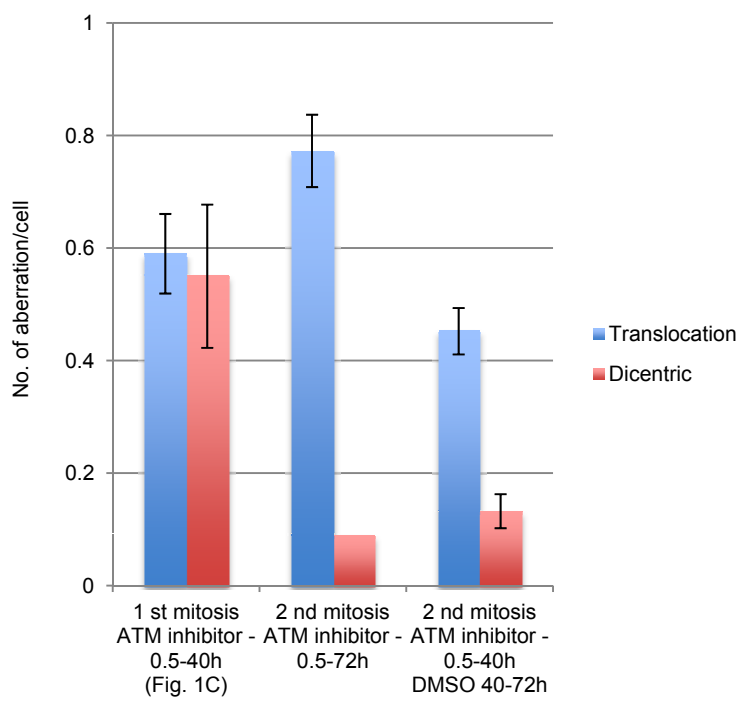

Supplementary Fig. 3

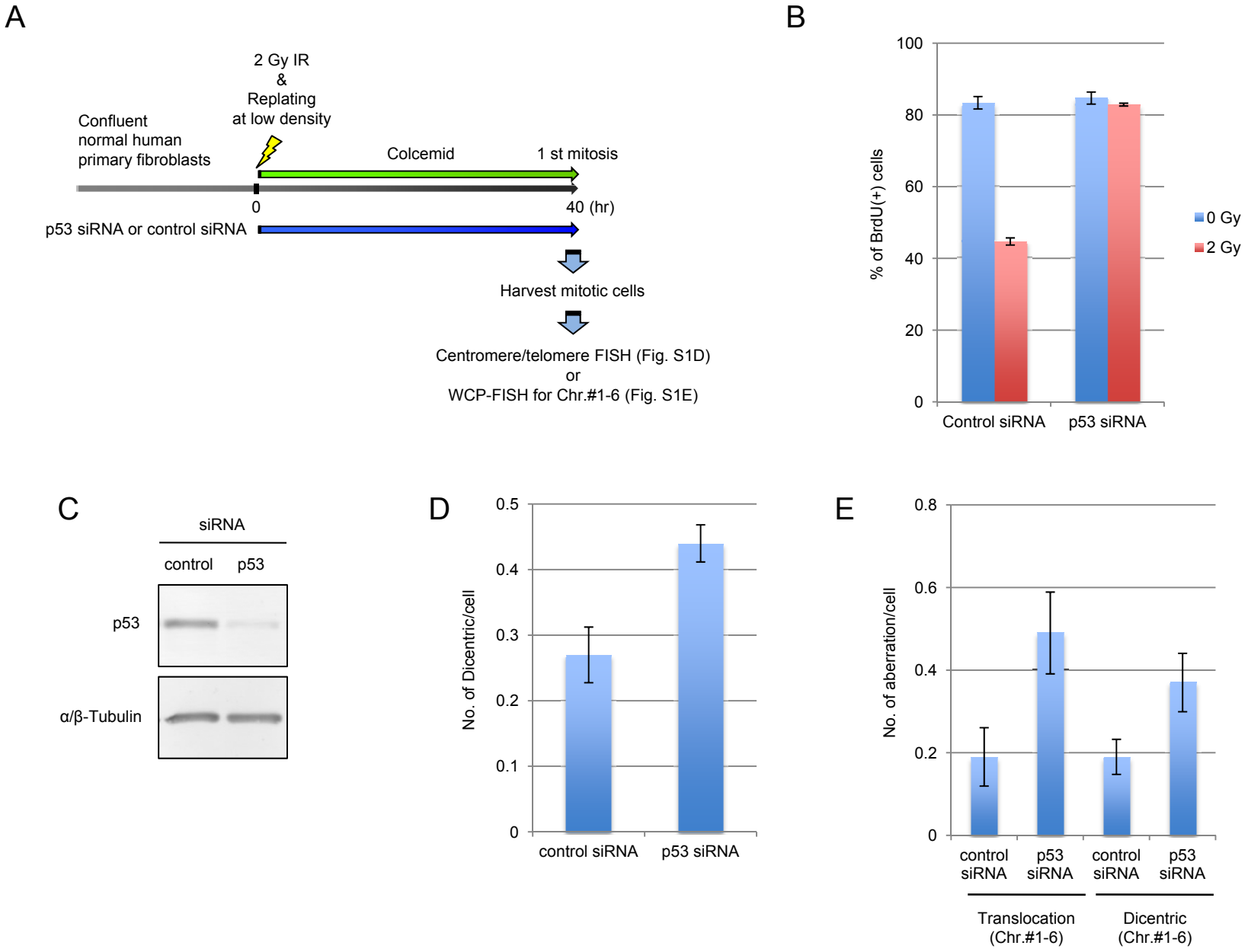

Supplementary Fig. 4

A

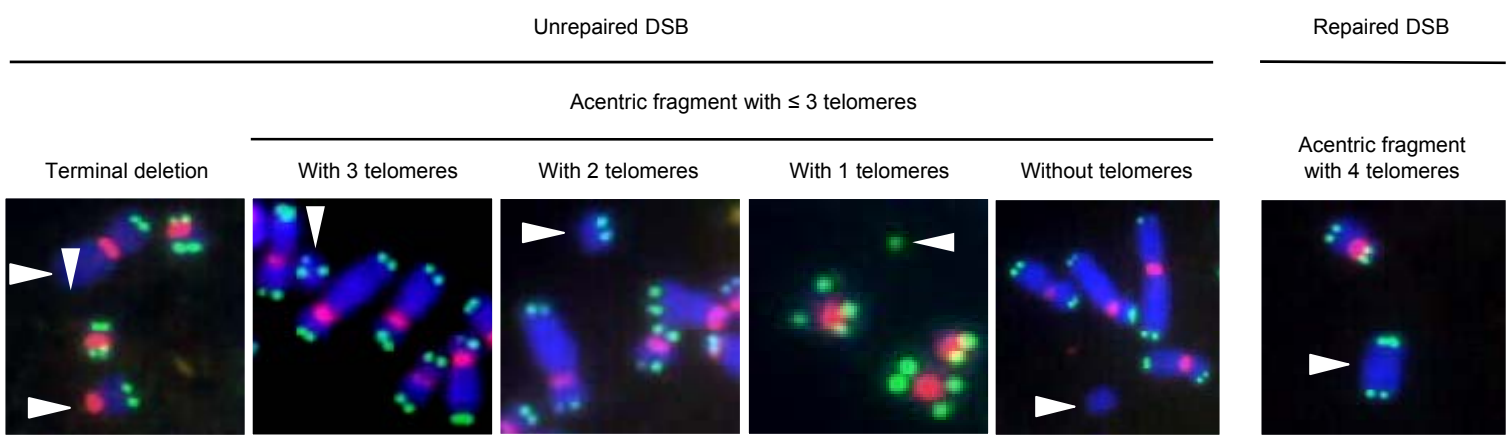

B